Astron. Astrophys. 324, 1170–1178 (1997)

ASTRONOMY
AND
ASTROPHYSICS

MHD surface type quasi-modes of a current sheet model

W.J. Tirry⋆**, V.M. Čadež, and M. Goossens**

Centre for Plasma Astrophysics, K.U.Leuven, Celestijnenlaan 200 B, B-3001 Heverlee, België

Received 9 December 1996 / Accepted 19 February 1997

Abstract. Resonantly damped surface type quasi-modes are computed as eigenmodes of the linear dissipative MHD equations for a simple equilibrium model of a current sheet. The current sheet is modeled by a nonuniform plasma layer embedded in a uniform plasma environment. The physical equilibrium variables change in a continuous way in the nonuniform plasma layer. In particular, this is the case with both the strength and the orientation of the equilibrium magnetic field resulting from an electric current in the nonuniform plasma layer. The equilibrium layer can be viewed as a model for a reconnection site in the solar atmosphere or for current sheets in the Earth's magnetosphere. Two surface type eigenmodes (kink and sausage) are numerically found that can propagate along the nonuniform plasma layer. The phase speeds of these eigenmodes are smaller than the Alfvén speed in the uniform environment. For oblique propagation to the equilibrium magnetic field, the eigenmodes resonantly couple to localized Alfvén waves leading to damped quasi-modes. It is shown that the wave damping is strongly anisotropic and that the dependence of the relative damping rate on the angle of propagation is different for the sausage and the kink type eigenmodes

Key words: magnetohydrodynamics (MHD) – methods: numerical – Sun: corona – Sun: oscillations

1. Introduction

Observations show the almost ubiquitous presence of magnetic structures in stellar atmospheres. The solar atmosphere is the best studied example of this intriguing physical behaviour.

The distribution of the magnetic field is not uniform with the magnetic field organized in typical structures in each part of the solar atmosphere. In the photosphere most of the magnetic flux outside active regions emerges from the network boundaries where it is concentrated by supergranulation flow in intense flux tubes. Since the plasma pressure drops off fast with height above the photosphere the intense flux tubes expand into the chromosphere and eventually fill out the whole volume of the upper chromosphere and the corona. In the corona the magnetic field is organized in closed magnetic loops and open magnetic regions. In the closed magnetic loops the magnetic field lines bend back and have two end points rooted in the dense photosphere. In the open magnetic regions the magnetic field lines extend into the heliosphere. The closed magnetic loops are seen as very bright and hot structures in X-ray observations. The open magnetic regions appear relatively dark and are known as coronal holes; here the plasma is flowing outward to give the fast solar wind.

Each of these magnetic structures can support MHD waves. Recent observations have revealed clear evidence of periodic (with a diversity of periods) and non-periodic oscillations (see e.g. Tsubaki 1988). MHD waves in the solar atmosphere are important in their own respect as they contain basic information about the equilibrium configurations in which they occur (see e.g. Roberts 1991). Therefore a good theoretical understanding of the relation between the frequencies and the physical quantities is required for MHD wave spectroscopy. MHD waves are also important because of their possible role for heating the solar corona.

Convective motions, global solar oscillations and local energy releases due to magnetic field reconnection are possible candidates for driving MHD waves. These MHD waves can then transport and deposit energy causing plasma heating.

A magnetic plasma region consisting of a region of low Alfvén speed surrounded by regions of high Alfvén speed is like a potential well for trapping magnetoacoustic waves (Roberts, Edwin & Benz 1984). This happens in a region of low magnetic field and/or high density surrounded by regions of strong magnetic field and/or low density. Coronal streamers containing both current sheets and closed dense loops present situations where ducted MHD waves can be anticipated. A similar situation which has attracted recent ample attention occurs in the chromospheric magnetic network. The magnetic field which extends out into the corona is rooted in the network defining the boundaries of the chromospheric supergranulation. Observations of the fine scale structure of the photospheric network suggest (Dowdy, Rabin & Moore 1986) a two component picture in which magnetic funnels that open into the corona emerge

Send offprint requests to: M. Goossens

⋆ Research Assistant of the F.W.O.-Vlaanderen

from only a fraction of the network. The remainder of the network is occupied by a population of low lying loops with length around 10^4 km (leading to a "magnetic junk yard" analogy according to Dowdy et al.). These loops constitute a source of magnetic energy. This energy can be tapped by magnetic field simplification of reconfiguration which results from reconnection events; i.e. microflares.

Recent observations by Falconer et al. (1996) suggest that microflaring might both directly heat the coronal plasma in the sheared local core field and generate waves that propagate into extended loops and dissipate there to produce the enhanced coronal heating in the bodies of these larger structures. The frequency spectrum of the waves by the network "microflares" is of considerable interest. The direct production of Alfvén waves by photospheric turbulence is criticized on the basis that there is an obvious mismatch between the low frequencies of the turbulent motions and the required high frequencies of the Alfvén waves (Parker 1992). Magnetic reconnection events as drivers of MHD waves do not face this difficulty because the periods of the waves that result from magnetic reconnection events are determined by the Alfvén speed and the geometry of the magnetic configuration involved, not by the characteristic periods of the turbulent motions. The reconfiguration of the magnetic field associated with a micro-flare converts very low frequency motions acting over a long time to high frequency motions generated over a short time.

An important property of MHD waves in an inhomogeneous plasma is that a global wave motion can be in resonance with local oscillations of a specific magnetic surface. The resonance condition is that the frequency of the global motion be equal to either the local Alfvén or the local cusp frequency of the magnetic surface. In this way energy is transferred from the large scale motion to oscillations which are highly localized to the neighbourhood of the Alfvén or cusp singular surface. In the dissipative MHD this behaviour is mathematically recovered as eigenmodes which are exponentially damped in time. Due to their global character (oscillating with the same frequency throughout the plasma) these modes are called 'global modes'. For ideal MHD such damped oscillations cannot be eigenmodes of the system, and for this reason they are often called 'quasi-modes' (see Tirry & Goossens 1996 and references therein). Since quasi-modes turn out to be global natural oscillations of the magnetic structures they will probably be most easily observed. It is therefore important to know how the frequencies of the quasi-modes are related to the distribution of the physical quantities and the geometry of the structure. For the same reason the quasi-mode plays a central role in the resonant absorption process as possible heating mechanism.

The focus of the present paper is on MHD quasi-modes in magnetic plasma structures where the magnetic field undergoes a rapid spatial variation in both strength and orientation and that, therefore, serve as MHD waveguides. Plenty of attention has been devoted to the theory of ducted MHD waves in plasmas with strong inhomogeneities. The early work, by Kruskal and Schwarzschild (1954), Ionson (1978), Uberoi (1972) that considered MHD surface modes propagating along a single discontinuity or a narrow transitional layer in magnetized plasmas, was followed by numerous investigations of surface waves along slabs (Roberts 1981; Edwin, Roberts & Hughes 1986), multilayered structures (Čadež & Okretič 1989), straight cylinders (Edwin & Roberts 1983), arcades (Smith, Roberts & Oliver 1997a), cylinders with a macroscopic fluid flow (Nakariakov, Roberts & Mann 1996) and structured current sheets (Smith, Roberts & Oliver 1997b).

In this paper we study ducted waves in the Harris neutral current sheet model (Harris 1962). Similar magnetic field structures can be found in regions where magnetic field reconnection processes might be possible like above active regions in the solar corona, in coronal streamers, in the chromospheric magnetic network and in planetary magnetospheres. We refer to Smith et al. (1997b) for references about frequently reported oscillations in the corona and the Earth's magnetosphere.

We show that the neutral current sheet model allows for two different types of surface modes to propagate along the domain of the pronounced inhomogeneity with the reduced magnetic field. They are of the sausage and the kink type respectively (Parker 1964), modified by possible local resonant effects in the presence of the continuous basic state profile. Numerical calculations of the eigenmode spectrum are performed for the case when the uniform part of the magnetic field B_0 is sufficiently strong, i.e. the related plasma β parameter will be taken to be zero. It is shown that only the Alfvén resonance can occur for the considered parameters while the condition for the slow resonance cannot be fulfilled for the obtained ducted modes. The Alfvén resonance occurs when the frequency of the surface mode matches the local Alfén frequency at some location known as the resonant point. The result is that the eigenfrequencies for the surface modes cannot be real, they have an additional negative imaginary part so that these waves are damped due to the resonant absorption. It is also shown that the wave damping is strongly anisotropic. If the propagation is along the magnetic field lines, then the Alfvén resonance disappears and the waves are classic eigenmodes with real frequencies.

The unperturbed initial configuration and the resistive MHD equations for linear motions are described in Sect. 2 and Sect. 3 respectively. The resonances and solutions are discussed in Sect. 4 while some of the details related to the numerical procedure are given in Sect. 5. Results and the summary are presented in Sect. 6 and Sect. 7 respectively.

2. The equilibrium configuration

We consider a static and magnetized plasma that is inhomogeneous along the $x-$axis with an electric current $\boldsymbol{j} = j_0(x)\hat{e}_y$ whose profile is given by

$$j_0(x) = \frac{j_{00}}{\mathrm{ch}^2(x/L)}, \qquad j_{00} = const. \tag{1}$$

This current is localized and has its maximal value j_{00} at $x = 0$ while the related magnetic field that follows from Ampere's

law $\mu_0 \boldsymbol{j}_0(x) = \nabla \times \boldsymbol{B}_0(x)$, is aligned along the $z-$ axis, $\boldsymbol{B}_0 = B_0(x)\hat{e}_z$ where:

$$B_0(x) = \mu_0 \int j_0(x)dx = B_{00}\text{th}(x/L) + B_{01}, \tag{2}$$

$B_{00} \equiv -\mu_0 j_{00} L$ and $B_{01} = const$ is the $z-$component of some background field existing in the absence of the current (1). We shall take $B_{01} = 0$ (as well as $B_{0x} = B_{0y} = 0$) which makes the field (2) antisymmetric with respect to $x = 0$ as it changes its orientation across the plasma layer with the localized current. The Harris neutral sheet models regions where magnetic field reconnection can occur: two practically homogeneous regions with magnetic fields of equal strength but with opposite orientations, are separated by a transitional layer of characteristic thickness L, where the field changes its strength and orientation.

The magnetic pressure distribution is symmetric with respect to $x = 0$: from the constant value $p_{m\infty}$ in the quasi-homogeneous region (at$|x/L| \gg 1$) it drops to zero at $x = 0$:

$$p_m(x) = p_{m\infty}\text{th}^2(x/L), \qquad p_{m\infty} \equiv \frac{B_{00}^2}{2\mu_0}. \tag{3}$$

The other plasma quantities, density $\rho_0(x)$ and temperature $T_0(x)$, should be specified in such a way that the condition of magnetohydrostatics is satisfied. When we neglect gravity, this means that the total pressure, the sum of the magnetic and the thermal pressure $p_0(x)$, is constant:

$$p_m(x) + p_0(x) = const \quad \text{and} \quad p_0(0) = p_{m\infty} + p_\infty. \tag{4}$$

Here p_∞ and $p_{m\infty}$ are the thermal and the magnetic pressure respectively, both taken at the quasi-homogeneous region $|x/L| \gg 1$.

The equilibrium condition (4) can be expressed as:

$$v_s^2(x)\rho_0(x) = \gamma[p_{m\infty}(1+\beta) - p_m(x)] \tag{5}$$

where the $p_m(x)$ is known and given by (3). The constant plasma-β_∞ parameter is defined as the ratio of the two pressures:

$$\beta_\infty \equiv \frac{p_\infty}{p_{m\infty}}.$$

and taken to be zero. Note that the local plasma β varies dramatically with x (being infinite at the current sheet centre).

The Alfvén speed, the cusp speed and the speed of sound are $x-$dependent and given by

$$v_A^2 = \frac{2p_m(x)}{\rho_0(x)}, \qquad v_C^2 = \frac{v_A^2 v_s^2}{v_A^2 + v_s^2},$$
$$v_s^2 = \gamma\frac{p_0(x)}{\rho_0(x)} \sim T_0(x)$$

where γ is the ratio of specific heats and taken to be $5/3$.

Relation (5) indicates that the distribution of one of the quantities, v_s^2 or ρ_0, can still be chosen freely. In our model, however, we shall assume a homogeneous density i.e. $\rho_0(x) \equiv \rho_0 = const$.

The Alfvén speed, the speed of sound and the cusp speed are then given by:

$$v_A^2 = v_{A\infty}^2\text{th}^2(x/L) \quad \text{where} \quad v_{A\infty}^2 \equiv 2\frac{p_{m\infty}}{\rho_0}, \tag{6}$$

$$v_s^2 = \frac{\gamma}{2}v_{A\infty}^2[1 + \beta - \text{th}^2(x/L)] \tag{7}$$

$$v_C^2 = \gamma v_{A\infty}^2\text{th}^2(x/L)\frac{1+\beta-\text{th}^2(x/L)}{\gamma(1+\beta)+(2-\gamma)\text{th}^2(x/L)} \tag{8}$$

The unperturbed plasma is taken to be ideal because the dissipative effects can be neglected on the time scale of the MHD wave propagation in the described basic state configuration.

The speed profiles (6-8) are plotted in Fig. 1. Lengths and speeds are normalised against the half-width L of the sheet and the Alfvén speed $v_{A\infty}$ in the exterior. Hence frequencies are measured in units of $v_{A\infty}/a$.

3. The linearized equations

In the presence of linear perturbations it is not any longer true that the plasma can be taken as ideal everywhere. We shall see that dissipation cannot be ignored near the possible resonant points due to the local quasi-singular behaviour of the solutions. In our model we shall include the Ohmic heating as the only dissipative mechanism and exclude the effects of viscosity and thermal conduction.

The standard set of linearized MHD equations for a resistive plasma is

$$\begin{aligned}
\frac{\partial \rho_1}{\partial t} + \nabla\cdot(\rho_0 \boldsymbol{v}_1) &= 0,\\
\rho_0\frac{\partial \boldsymbol{v}_1}{\partial t} &= -\nabla p_1 + \frac{1}{\mu_0}(\nabla\times\boldsymbol{B}_1)\times\boldsymbol{B}_0\\
&\quad + \frac{1}{\mu_0}(\nabla\times\boldsymbol{B}_0)\times\boldsymbol{B}_1,\\
\frac{\partial \boldsymbol{B}_1}{\partial t} &= \nabla\times(\boldsymbol{v}_1\times\boldsymbol{B}_0) + \eta\nabla^2\boldsymbol{B}_1\\
\frac{\partial p_1}{\partial t} + \boldsymbol{v}_1\cdot\nabla p_0 &= v_s^2(\frac{\partial \rho_1}{\partial t} + \boldsymbol{v}_1\cdot\nabla\rho_0)
\end{aligned} \tag{9}$$

The perturbed quantities f_1 are then Fourier analyzed with respect to y, z and t. The amplitudes of the corresponding Fourier components remain $x-$dependent:

$$f_1(x,y,z,t) = f(k_y,k_z,\omega,x)\text{e}^{i(k_y y + k_z z - \omega t)}.$$

Because of the very high values of the magnetic Reynolds number for the solar coronal conditions, the dissipation due to the finite electrical resistivity η can be ignored except in narrow layers of steep gradients (e.g. around resonances). Outside these dissipative layers the Eqs. (9) reduce to the following two coupled first order differential equations for the perturbations of the normal component of the Lagrangian displacement $\xi_x \equiv -i\omega v_x$ and of the total pressure perturbation P (see Appert et al. 1974):

$$D\frac{d\xi_x}{dx} = -C_1 P, \qquad \frac{dP}{dx} = C_2\xi_x \tag{10}$$

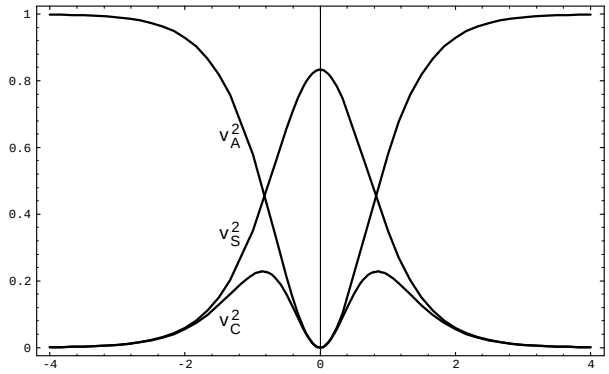

Fig. 1. Profiles of the characteristic speeds (squared): the Alfvén $v_A^2(x)$, the sound $v_s^2(x)$ and the cusp $v_C^2(x)$.

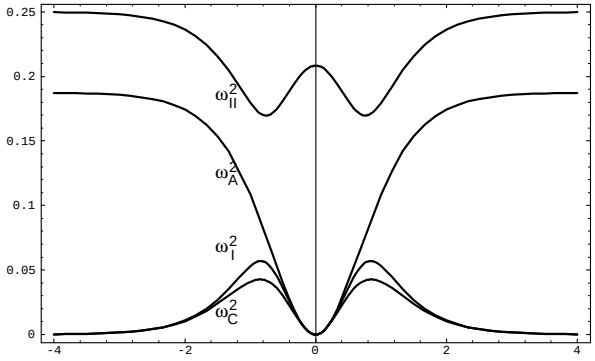

Fig. 2. Typical profiles of characteristic frequencies (squared) : the upper cutoff $\omega_{II}^2(x)$, the Alfvén $\omega_A^2(x)$, the lower cutoff $\omega_I^2(x)$ and the cusp $\omega_C^2(x)$ for $k = 0.5$ and $\theta = 30^o$.

where

$$D = \rho_0(v_s^2 + v_A^2)(\omega^2 - \omega_C^2)(\omega^2 - \omega_A^2),$$

$$C_1 = (\omega^2 - \omega_A^2)(\omega^2 - \omega_s^2) - \omega^2 v_A^2 k_y^2,$$

$$C_2 = \rho_0(\omega^2 - \omega_A^2)$$

and

$$\omega_A = v_A k_z, \qquad \omega_s = v_s\sqrt{k_y^2 + k_z^2}, \qquad \omega_C = v_C k_z.$$

C_1 can be rewritten as

$$C_1 = (\omega^2 - \omega_I^2)(\omega^2 - \omega_{II}^2)$$

where ω_I and ω_{II} are known as the cut-off frequencies.

4. Dissipative solutions around the resonances

Eqs. (10) are singular at locations where the coefficient D vanishes, i.e. when either of the two conditions

$$\omega = \omega_A(x_A) \qquad \text{or} \qquad \omega = \omega_C(x_C), \tag{11}$$

is satisfied either at $x = x_A$ (the Alfvén resonance) or at $x = x_C$ (the cusp or the slow resonance) respectively. The frequency matching (11) indicates a resonant wave transformation due to the excitation of either a local Alfvén wave or a local slow MHD wave. As a consequence, the perturbation amplitudes and their spatial derivatives diverge at the resonant positions in an ideal plasma. In reality this can not happen due to the dissipative processes that become important in some vicinity $\pm d_\eta$ around the resonant points x_C and x_A.

A full theory concerning the processes in the dissipative layer around a resonance was developed by Sakurai, Goossens and Hollweg (1991) and Goossens et al. (1995a,b) for the driven problem. The solution inside the dissipative layer for the eigenvalue problem was for the first time determined analytically by Ruderman, Tirry and Goossens (1995) for resonantly damped Alfvén surface waves in a resistive and viscous plasma with incompressible motions. Tirry and Goossens (1996) considered the more general case of coupling between global compressional modes and localized Alfvén waves.

The overall solutions for ξ_x and P are now obtained by solving the ideal Eqs. (10) outside the dissipative layers and the dissipative equations (9) inside the layers with the requirement for continuous solutions at the boundaries of the layers. Since dissipation is effective in the close vicinity of the resonant points only, we can simplify the initial set of equations (9) by reducing them first to a form analogous to (10) and then express the coefficients as linear functions of the distance s from the resonant point. Due to the resonant coupling to localized waves, the waves are damped and therefore their eigenfrequencies are complex: $\omega = \omega_r + i\omega_i$.

In the case of the Alfvén resonance at $s \equiv x - x_A = 0$ the Eqs. (9) can be approximated in some interval $[-s_A, +s_A]$ around the resonance, by the following set

$$\left[2i\omega_A\omega_i + s\Delta_A - i\omega_A\eta\frac{d^2}{ds^2}\right]\frac{d\xi_x}{ds}$$

$$= -\left[\frac{(2i\omega_A\omega_i + s\Delta_A)(\omega_A^2 - k_z^2 v_s^2)}{\rho_0(v_s^2 + v_A^2)(\omega_A^2 - \omega_C^2)} - \frac{k_y^2}{\rho_0}\right]P \tag{12}$$

$$\frac{dP}{ds} = \rho_0(2i\omega_A\omega_i + s\Delta_A)\xi_x$$

where $\Delta_A \equiv (d/ds)(\omega^2 - \omega_A^2)$. The coefficients are evaluated at $s = 0$ and $|\omega_i| \ll |\omega_A|$ (or a weak wave damping) is assumed but this has to be checked a posteriori when the solutions are obtained. In the numerical code the resistivity η is assumed to be important only inside the narrow dissipative layer $[-d_{\eta A}, +d_{\eta A}]$ whose half-thickness $d_{\eta A}$ is evaluated in our calculations as $d_{\eta A} \approx 5 \times \delta_A$ where

$$\delta_A = \left(\frac{\omega\eta}{|\Delta_A|}\right)^{1/3} \ll s_A$$

defines the length scale of the resonance layer as can be estimated from the first equation in (12).

In Eqs. (12) the highest derivative term is multiplied with the electrical resistivity. Hence for very high Reynolds numbers,

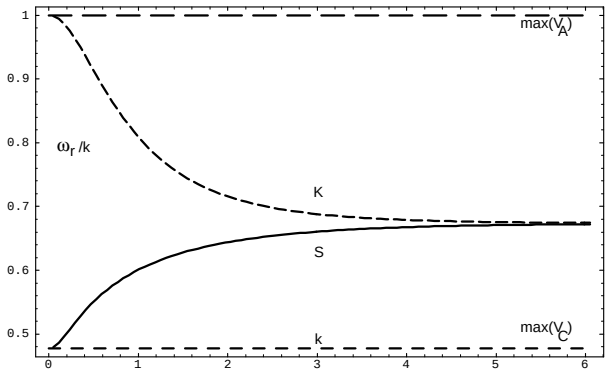

Fig. 3. The dispersion curves for the kink (K) and the sausage (S) surface mode propagating along the magnetic field.

Eqs. (12) represents a singular perturbation problem. Now it is convenient to introduce a new scaled variable $\tau = s/\delta_A$ which is of the order 1 in the dissipative layer. With this new variable the Eqs. (12) for ξ_x and P take the form:

$$\left[\frac{d^2}{d\tau^2} + i\,\mathrm{sign}(\Delta_A)\tau - \Lambda\right]\frac{d\xi_x}{d\tau}$$

$$= -\left\{\delta_A \frac{[-\Lambda + i\mathrm{sign}(\Delta_A)\tau](\omega_A^2 - k_z^2 v_s^2)}{\rho_0(v_s^2+v_A^2)(\omega_A^2-\omega_C^2)} - i\frac{k_y^2}{\rho_0|\Delta_A|}\right\}P$$

$$\frac{dP}{d\tau} = -i\delta_A^2\rho(x_A)|\Delta_A|[-\Lambda + i\mathrm{sign}(\Delta_A)\tau]\xi_x \qquad (13)$$

where $\Lambda = 2\omega_A\omega_i/(\delta_A|\Delta_A|)$. Hence, in the zeroth order, the total pressure perturbation P is a conserved quantity across the resonance layer and an analytical solution for ξ_x can be found (see Tirry & Goossens 1996) in the following form:

$$\xi_x(\tau) = -\left[\frac{\delta_A(\omega_A^2 - k_z^2 v_s^2)\tau}{\rho_0(v_s^2+v_A^2)(\omega_A^2-\omega_C^2)} - \frac{k_y^2 G(\tau)}{\rho_0\Delta_A}\right]C_A + C_1$$

$$P(\tau) = C_A \qquad (14)$$

where

$$G(\tau) = \int_0^\infty \left[e^{iu\mathrm{sign}(\Delta_A)\tau - \Lambda u} - 1\right] e^{\frac{-u^3}{3}}\frac{du}{u}.$$

and C_A and C_1 are constants of integration.

In the case of the slow resonance, the analysis is analogous and the outcome for the solution in the corresponding dissipative layer is

$$\xi_x(\tau) = \frac{C_1 C_C}{\rho_0\Delta_C(v_s^2+v_A^2)(\omega_C^2-\omega_A^2)}G(\tau) + C_2$$

$$P(\tau) = C_C \qquad (15)$$

where $\Delta_C \equiv (d/ds)(\omega^2 - \omega_C^2)$ and C_C and C_2 are contants of integration. The coefficients are evaluated now at the slow (the cusp) resonance $s \equiv x - x_C = 0$. We shall use our solutions (14) and (15) in numerical calculations for solving the eigenvalue problem of MHD surface waves on the current carrying layer.

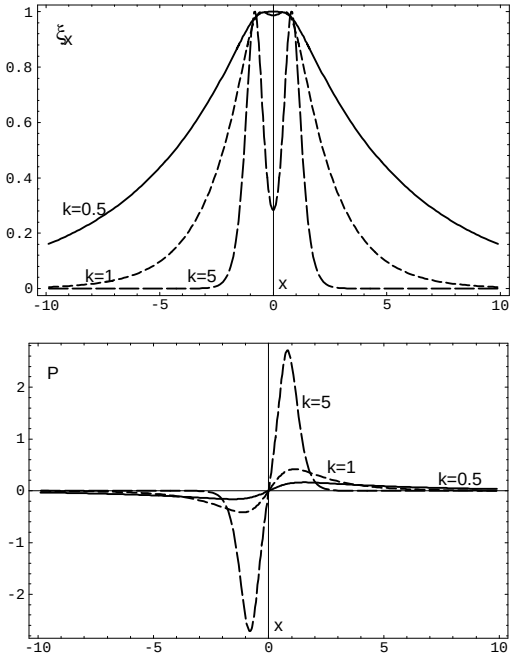

Fig. 4. The solutions for the normal displacement ξ_x and the total pressure perturbation P for the kink mode propagating along the magnetic field ($k_y = 0$). Here: $k = k_z = 0.5$, 1 and 5.

5. Numerical procedure

The eigenvalue problem is solved numerically making use of the fact that a symmetric basic state profile (6-8) allows only symmetric and antisymmetric solutions for ξ_x and P. The antisymmetric solution for ξ_x vanishes and changes its sign when crossing $x = 0$ while P has an extremum there, according to Eqs. (10). This solution represents the sausage mode with plasma being at rest along the plane $x = 0$ and oscillating with equal speeds in opposite directions at symmetric points $\pm x$. Similarly, the symmetric solution for ξ_x is the kink mode with the total pressure perturbation $P = 0$ at $x = 0$.

The equilibrium state has the property that it is uniform for all practical purposes if $|x|/L \geq 10$. For the MHD eigenoscillations this implies that they have spatially oscillatory behaviour where the corresponding frequency satisfies the wave propagation conditions $\omega > \omega_{II}(\infty)$ or $\omega_I(\infty) > \omega > \omega_C(\infty)$. Otherwise the spatial behaviour is non-oscillatory. Here $\omega_I(\infty)$, $\omega_{II}(\infty)$ and $\omega_C(\infty)$ are the lower cutoff, the upper cutoff and the cusp frequency respectively all taken at large x/L, i.e. at $|x|/L \geq 10$ in the present case.

Since we are primarily interested in localized surface type modes, with evanescent amplitudes at large distances $|x/L| \geq 10$, the related frequencies should lie in the intervals

$$\omega_{II}(\infty) > \omega > \omega_I(\infty) \quad \text{or} \quad \omega_C(\infty) > \omega. \qquad (16)$$

The numerical calculations are performed with dimensionless quantities, $\beta = 0$ and $\eta = 10^{-6}$. The starting point for the numerical integration of (10) is $x = -10$ where the plasma is

uniform. The analytical evanescent solution of (10) valid for $x \leq -10$ is simply

$$P(x) = A\mathrm{e}^{\kappa x} \quad \text{and} \quad \xi_x(x) = A\frac{\kappa}{C_2}\mathrm{e}^{\kappa x} \tag{17}$$

where $\kappa = \sqrt{-C_1C_2/D}$. All coefficients are evaluated at $x = -10$. The arbitrary complex factor A is taken to be (1,1).

Thus the procedure of solving the eigenvalue problem is a shooting method. When the initial set of parameters $\{k_y, k_z, \omega\}$ with the frequency ω in the intervals given by (16) is prescribed, the initial values $P_0 \equiv P(-10)$ and $\xi_0 \equiv \xi_x(-10)$ follow from (17). Starting from P_0 and ξ_0, we numerically integrate the ideal MHD Eqs. (10) towards $x = 0$ using a fourth order Runga-Kutta method. If a resonance is encountered during the calculation, then the dissipative solutions (14) or (15) are applied continuously between the end points $\pm 5\delta_{A,C}$ of the corresponding dissipative layer. After having passed through the dissipative layer the computations return to the ideal Eqs. (10) until the final point $x = 0$ is reached. The resulted values for P and ξ at $x = 0$ are now meaningful only if one of them vanishes according to the earlier conclusion about solutions being either symmetric or antisymmetric. Otherwise, a new value for ω is taken while keeping k_y and k_z fixed and the whole procedure is repeated. The spectra for the surface modes follow as complex roots of the functions:

$$\xi_x(0) = 0 \quad \text{or} \quad P(0) = 0 \tag{18}$$

for the sausage or the kink mode respectively.

6. Results

In Fig. 2 the typical profiles of the characteristic frequencies ω_A^2, ω_C^2, ω_I^2 and ω_{II}^2 are plotted for $k \equiv \sqrt{k_y^2 + k_z^2} = 0.5$ and with the angle of propagation (with respect to the magnetic field $\boldsymbol{B}_0$) $\theta = 30^o$. The related wave vector components are then $k_y = k\sin(\theta)$ and $k_z = k\cos(\theta)$. If $k_y \to 0$ the cutoff frequencies ω_I and ω_{II} approach ω_s and ω_A. The case $k_y = 0$ is extensively studied by Smith, Roberts & Oliver (1997b). The current sheet supports waves which may be body, surface or hybrid modes. The terms body and surface refer to oscillatory and non-oscillatory behaviour in the current sheet structure respectively while the term hybrid refers to a mixture of body and surface wave properties. By examination of the driving forces and perturbed pressures Smith et al. (1997b) show that no purely fast or slow modes exist but that the eigenmodes have a mixed character.

In this paper we call the modes surface type modes although they can be body or hybrid according to the terminology used by Smith et al.. In addition we will focus on the fundamental kink and sausage mode with characteristic frequencies in the Alfvén continuum. Higher harmonics which appear above certain wave number cut-offs (Edwin, Roberts & Hughes 1986) are not considered here.

In what follows we first consider the case of parallel propagation ($k_y = 0$). How the spectrum of the surface waves is altered when $k_y \neq 0$, is investigated in the third paragraph.

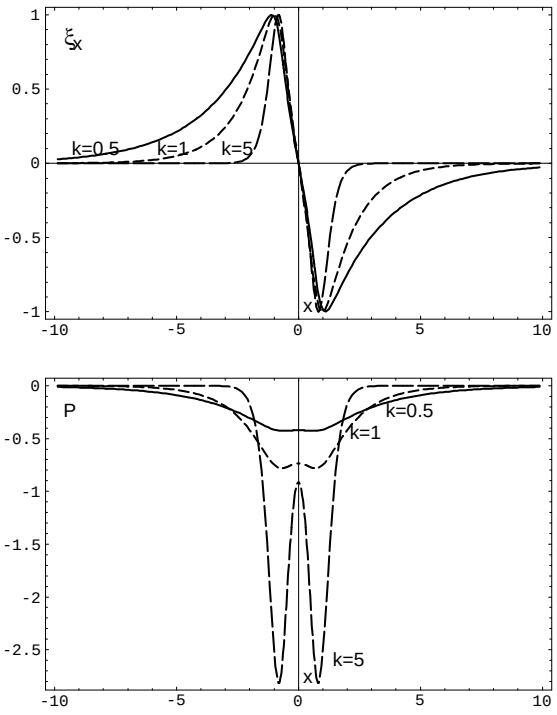

Fig. 5. The solutions for the normal displacement ξ_x and the total pressure perturbation P for the sausage mode propagating along the magnetic field ($k_y = 0$). Here: $k = k_z = 0.5$, 1 and 5.

Parallel propagation For $k_y = 0$, there is no Alfvén singularity in the ideal MHD Eqs. (10). This means that possible surface wave propagating along the magnetic field cannot resonantly excite local Alfvén waves.

The numerical solutions of (18) show that the fundamental kink and sausage modes exist for all values of the wave number. In the long wave length limit the phase speeds of the kink and sausage mode approach the maximum value of the Alfvén speed and the tube speed respectively. Both eigenfrequencies are real and lie in the domain between the corresponding cut-offs $\omega_I(\infty)$ and $\omega_{II}(\infty)$. According to Fig. 2, this means that the slow resonance can not occur either.

Thus the waves propagating along the magnetic field or along the inhomogeneous slab, are not affected by dissipation and they are the classic eigenmodes with real eigenfrequencies. Their dispersion properties are shown in Fig. 3. The phase speeds are smaller than the Alfvén speed $v_{A\infty}$ in the uniform environment (Edwin & Roberts 1982) and they converge to each other at larger values of k_z.

The corresponding eigenfunctions for the total pressure perturbation P and the normal displacement ξ_x are shown in Fig. 4 and Fig. 5 for the kink and the sausage mode respectively, for three different values of k_z: 0.5, 1 and 5. The eigenfunctions are normalised with respect to the maximum value in ξ_x. A general property of these solutions is that their localized profiles tend to broaden when k_z decreases i.e. when the wavelength is increasing. This means that surface waves with relatively longer wavelengths can still be detected at locations where the plasma

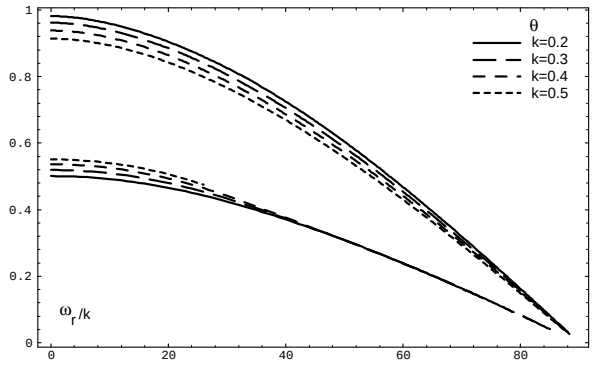

Fig. 6. The oscillation frequency ω_r as function of the angle of propagation for the kink and the surface fundamental mode.

is quasi-homogeneous. On the other hand the waves with relatively shorter wavelengths are more concentrated near that part of the inhomogeneous plasma layer where the basic state quantities have large gradients. As k_z increases the oscillations become more localised about the edges of the sheet (see e.g. Smith et al. 1997b).

Oblique propagation When $k_y \neq 0$, the ideal MHD Eqs. (10) are now singular at the location where the frequency matches the local Alfvén frequency. The two fundamental surface modes (the kink as the sausage mode) then resonantly couple to localized Alfvén waves leading to damped surface type quasi-modes with a complex eigenfrequency $\omega = \omega_r + i\omega_i$.

Fig. 6 shows the decrease of the oscillation eigenfrequency with an increase of the angle of propagation for both considered quasi-modes with $k = 0.2, 0.3, 0.4, 0.5$. In the limit $\theta \rightarrow 90^o$ ($k_z \rightarrow 0$) the modes stop to exist as the Alfvén continuum shrinks to zero. The wave frequencies ω_r of both quasi-modes are always higher than the maximal value of ω_C. Hence, the slow resonance does not occur.

Fig. 7a and Fig. 7b show how the relative damping rate ω_i/ω_r vary with the angle θ for several values of the wave number k for the fundamental kink and sausage surface mode respectively. These plots indicate, first of all, that we really have quasi-modes with the condition $|\omega_i| \ll \omega_r$ satisfied in the range of the parameter values used in the computations. For the sausage mode we see an increase of $|\omega_i/\omega_r|$ at lower angles, reaching an extremum at some θ and decreasing afterwards at higher values of θ. The higher the value of the wave number k the higher the relative damping rate is.

For the kink type mode a totally different dependence of the relative damping rate on the angle of propagation is found. There is a steady increase in the damping rate with the angle θ. At a certain angle (depending on the value of the wavenumber) the relative damping rate is too high and the width δ_A of the resonance layer is too large (the resonance position shifts towards the interval where the Alfvén frequency is almost constant ($\Delta_A \rightarrow 0$)) for our local analysis described in Sect. 4 to remain valid. For this reason our calculations do not go beyond the values shown in Fig. 7a and 7b. The increase in relative

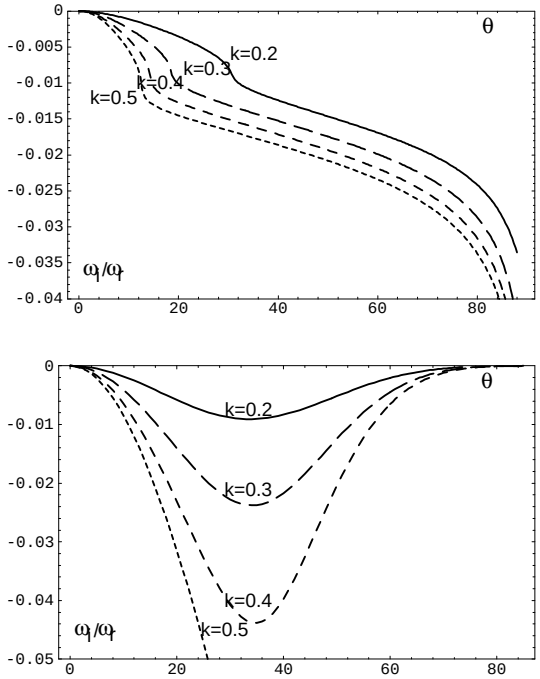

Fig. 7. The relative damping rate ω_i/ω_r as function of the angle of propagation for the kink (upper plot) and the sausage (lower plot) fundamental mode.

damping rate is not purely monotonic around a certain angle. The nature of the kink mode evolves along the curve from a body mode through a hybrid to a pure surface mode. As mentioned, it is the Alfvén resonance that causes the wave dissipation and that is responsible for the complex eigenfrequencies. How this resonance affects the solutions for P and ξ_x for each of the two quasi-modes is seen in Fig. 8a for the kink mode and in Fig. 8b for the sausage mode. The waves are taken to propagate at $\theta = 15^o$ for the kink mode and $\theta = 20^o$ for the sausage mode with the wave number $k = 0.4$. The Alfvén resonance is clearly seen in these figures. The narrow dissipative layer is characterized by rapidly alternating solutions with the number of peaks increasing (and amplitude growing) with increasing relative damping rate as shown enlarged in Fig. 9 for the fundamental kink mode when $\theta = 15^o, 20^o$.

7. Summary

In this paper quasi-modes are computed in a current sheet model as eigenmodes (surface modes) of the linear dissipative MHD equations. The quasi-mode manifests itself as a natural coherent oscillation and therefore it is very important for MHD wave spectroscopy. Since the quasi-mode represents a coupling between a global oscillation and a localized continuum mode (with an energy transfer form the global mode towards the local mode) it can play an important role in the resonant absorption process as heating mechanism by waves.

For example, these quasi-modes could be important in a DC/AC hybrid heating mechanism in the two-component pic-

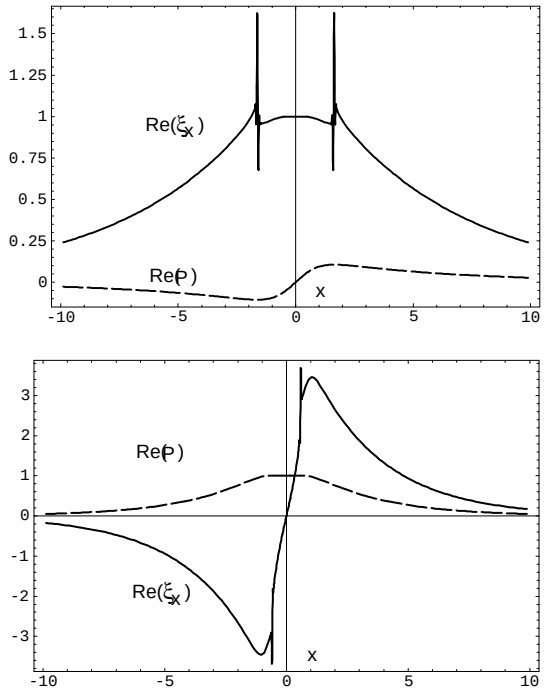

Fig. 8. The spatial distributions of the real parts of P and ξ_x for the kink (upper plot) and the sausage (lower plot) mode with wave number $k = 0.4$, $\theta = 15^o$ for the kink mode and $\theta = 20^o$ for the sausage mode.

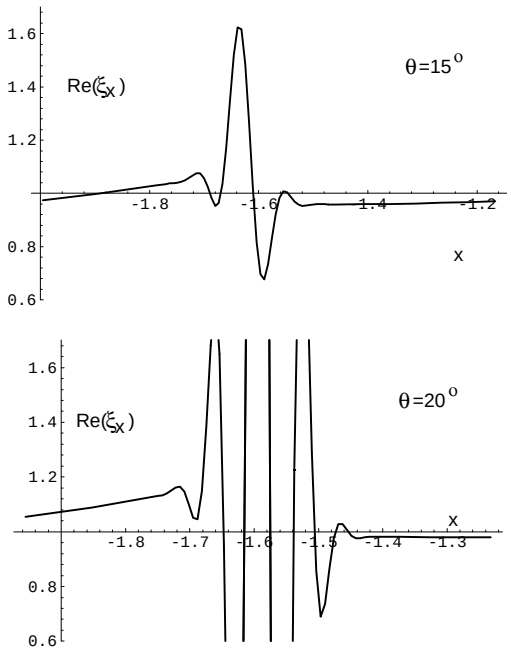

Fig. 9. The solutions $Re(\xi_x)$ inside the dissipative layer for the kink mode for two angles of propagation: $\theta = 15^o, 20^o$.

ture (magnetic funnels together with a junk yard of low lying loops) of the chromospheric magnetic network: microflaring may produce local chromospheric heating by DC dissipation and at the same time trigger MHD quasi-modes in the junk yard of magnetic loops and current sheets.

The eigenmode computation is carried out with a simple numerical scheme: using the analytical solution inside the dissipative layer to cross the quasi-singular resonance layer. The required numerical effort is limited to the integration of the ideal MHD equations in regions away from any singularity.

In the case of propagation parallel to the magnetic field ($k_y = 0$) two different surface type modes on the nonuniform plasma layer are found: the sausage and the kink type. The phase speeds of these fundamental eigenmodes are smaller than the Alfvén speed in the uniform environment and merge into each other for large values of the wavenumber k_z where they remain constant.

These modes can also propagate under some angle θ to the magnetic field, but then they are damped due to the resonant coupling to the localized Alfvén waves. No modes are found in the slow continuum. Cramer (1994) investigated magneto-acoustic surface waves for current sheets in which the magnetic field rotates with constant amplitude, so that the gas pressure remains constant. He found that the Alfvén resonance damping always occurs, as well as (for high β and certain angles of propagation) the slow resonance damping.

The dependence on the angle θ can be summarized as follows : for the sausage mode there is a rapid increase in damping rate with increasing θ which is more pronounced at higher oscillation frequencies; at certain angle a maximum damping rate (coupling) is reached, followed by a decrease for higher values of θ. On the other hand for the kink mode we see a steady increase in relative damping rate.

The equilibrium current carrying layer can be viewed as a model of a reconnection site in regions both in the solar atmosphere as in the Earth's magnetosphere. For solar corona applications the periods of the fundamental eigenmodes are of the order of seconds (see e.g. Smith et al. 1997b). As noted by Smith et al. periods of this order are frequently reported (Aschwanden 1987; Zlobec et al. 1992; Pasachoff & Landman 1984; Pasachoff & Ladd 1987; Zhao et al. 1990; Aschwanden et al. 1994; Karlický & Jiřička 1995). For the Earth's magnetosphere the periods are of the order of minutes. Therefore the 1-2 minute magnetic field fluctuations of the neutral sheet observed by Bauer et al. (1995a,b) may indeed be due to waves propagating in a neutral sheet.

The current sheets are mostly likely to be accompanied with mass flows. It is important therefore to investigate what happens with the MHD surface type quasi-modes on a current sheet in presence of a mass flow. This will be done in a forthcoming paper which also will include a parametric study relevant for application to regions in the solar atmosphere and the Earth's magnetosphere.

Acknowledgements. The authors are grateful to the referee B. Roberts for his comments and suggestions for the revision of the original manuscript. V. M. Čadež acknowledges the financial support by the 'Onderzoeksfonds K.U.Leuven' (the senior research fellowship F/95/62) and thanks the colleagues from CPA for a friendly and highly professional environment.

References

Appert, K., Gruber, R., & Vaclavik, J. 1974, Phys. Fluids, 17, 1471
Aschwanden, M.J. 1987, SPh, 111, 113
Aschwanden, M.J., Benz, A.O., Dennis, B.R., & Kundu, M.R. 1994, ApJ (SS) 90, 631
Bauer, T.M., Baumjohann, W., & Treumann, R.A. 1995a, J. Geophys. Res. 100, 23737
Bauer, T.M., Baumjohann, W., Treumann, R.A., Sckopke, N., & Lühr, H. 1995b, J. Geophys. Res. 100, 9605
Čadež, V.M. & Okretič, V.K. 1989, J.Plasma Physics, 41, 23
Cramer, N.F. 1994, J. Plasma Physics, 51(2), 221
Dowdy, J.F., Rabin, D., & Moore, R.L. 1986, SPh, 105, 35
Edwin, P. & Roberts, B. 1982, SPh 76, 239
Edwin, P., & Roberts, B. 1983, SPh, 88, 179
Edwin, P., Roberts, B., & Hughes, W.J. 1986, Geophys. Res. Letters 13, 373
Falconer, D.A., Moore, R.L., Porter, J.G., Gary, G.A., & Shimizu, T. 1996, ApJ, in press
Goossens, M., Ruderman, M.S., & Hollweg, J. 1995a, SPh, 157, 75
Goossens, M., & Ruderman, M.S. 1995b, Physica Scripta, T60, 171
Harris, E. 1962, Nuovo Cim. 23, 115
Ionson, J.A. 1978, ApJ, 226, 650
Karlický, M., & Jiřička, K. 1995, SPh 160, 121
Kruskal, M., & Schwarzschild, M. 1954, Proc.Roy.Soc.Lond., A223, 348
Nakariakov, V.M., Roberts, B., & Mann,G. 1996, A&A, 311, 311
Parker,E.N. 1964, ApJ, 139, 690
Parker,E.N. 1992, J. Geophys. Res., 97, 4311
Pasachoff, J.M., & Landman, D.A. 1984, SPh 90, 325
Pasachoff, J.M., & Ladd, E.F. 1987, SPh 109, 365
Roberts, B. 1981, SPh, 69, 39
Roberts, B., Edwin, P., & Benz, A.O. 1984, ApJ 279, 857
Roberts, B. 1991, in Advances in Solar System Magnetohydrodynamics, ed. E.R. Priest, & A.W. Hood (New York:Cambridge Univ. Press), 105
Ruderman, M.S., Tirry, W.J. & Goossens, M. 1995, J.Plasma Physics, 54, 129
Sakurai, T., Goossens, M., & Hollweg,J.V. 1991, SPh, 133, 227
Smith, J.M.,Roberts, B., & Oliver, R.: 1997a, A&A, 317, 752
Smith, J.M.,Roberts, B., & Oliver, R.: 1997b, A&A, submitted
Tirry, W.J., & Goossens, M. 1996, ApJ, 471, 501
Tsubaki, T. 1988, in Solar and Stellar Coronal Structures and Dynamics, ed. Altrock, R.C.,140
Uberoi, C. 1972, Phys.Fluids, 15, 1673.
Zhao, R-Y., Jun, S-Z., Fu, Q-J., & Li, X-C. 1990, SPh 130, 151
Zlobec, P., Messerotti, M., Dulk, G.A., & Kucera, T. 1992, SPh 141, 165

This article was processed by the author using Springer-Verlag LaTeX A&A style file *L-AA* version 3.